

Modular assembly of porous organic cage crystals: Isoreticular quasiracemates and ternary co-crystal

Srinu Tothadi, Marc A. Little, Tom Hasell, Michael E. Briggs, Samantha Y. Chong, Ming Liu, and Andrew I. Cooper*

This document contains Supplementary Figures, S1-S13.

1. Characterization and Supporting figures

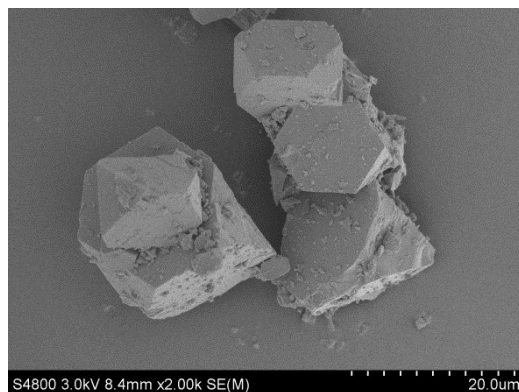


Figure S1. SEM images of quasiracemate, $(\text{FT-RCC3-R})\cdot(\text{CC1-S})$, crystallised from $\text{CH}_2\text{Cl}_2/\text{acetone}$.

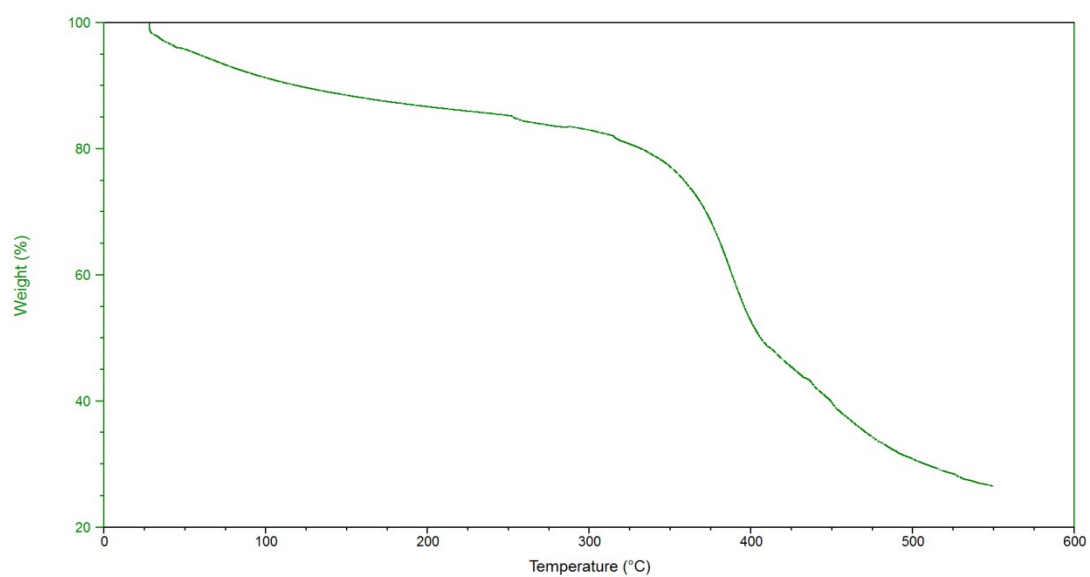


Figure S2: TGA of quasiracemate, $(\text{FT-RCC3-R})\cdot(\text{CC1-S})$, crystallised from $\text{CH}_2\text{Cl}_2/\text{acetone}$.

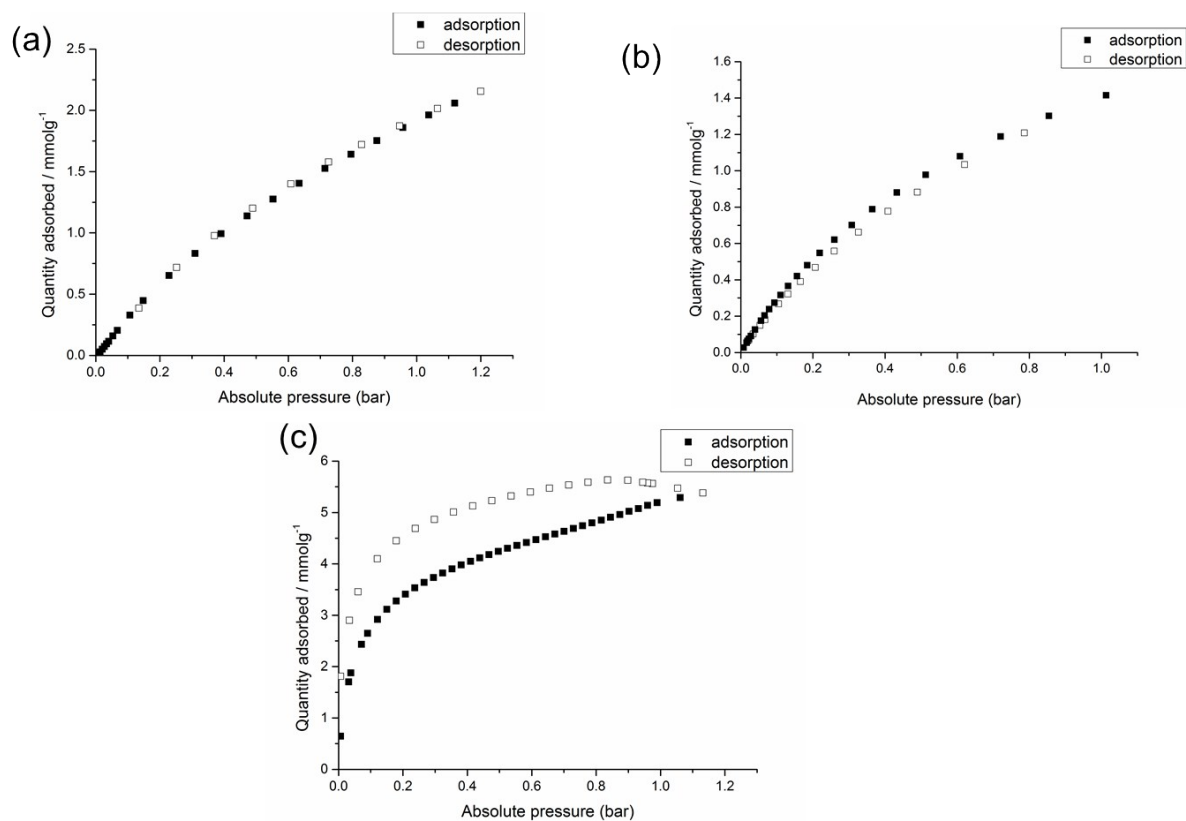


Figure S3. Gas sorption isotherms of quasiracemate, $(\text{FT-RCC3-R})\cdot(\text{CC1-S})$, (a) CO_2 at 278 K, (b) CH_4 at 278 K, and (c) H_2 at 77 K. $(\text{FT-RCC3-R})\cdot(\text{CC1-S})$ was crystallised from $\text{CH}_2\text{Cl}_2/\text{acetone}$ and activated by heating under vacuum at 90 °C. Closed and open symbols represent adsorption and desorption curves, respectively.

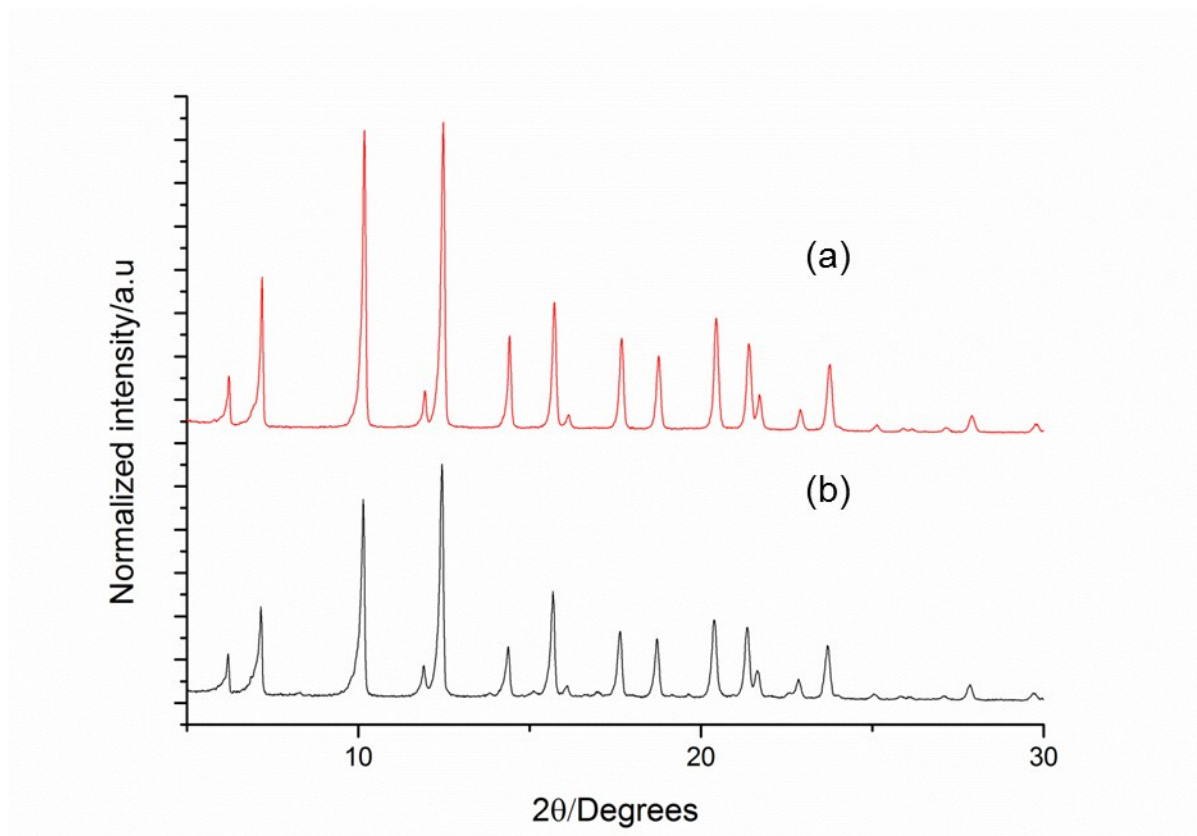


Figure S4. PXRD for quasiracemate, $(\text{FT-RCC3-R})\cdot(\text{CC1-S})$, recorded (a) before, and (b) after gas sorption. There is no phase change during gas sorption analysis indicating the materials is stable. Crystals obtained from DCM/Acetone (anti-solvent).

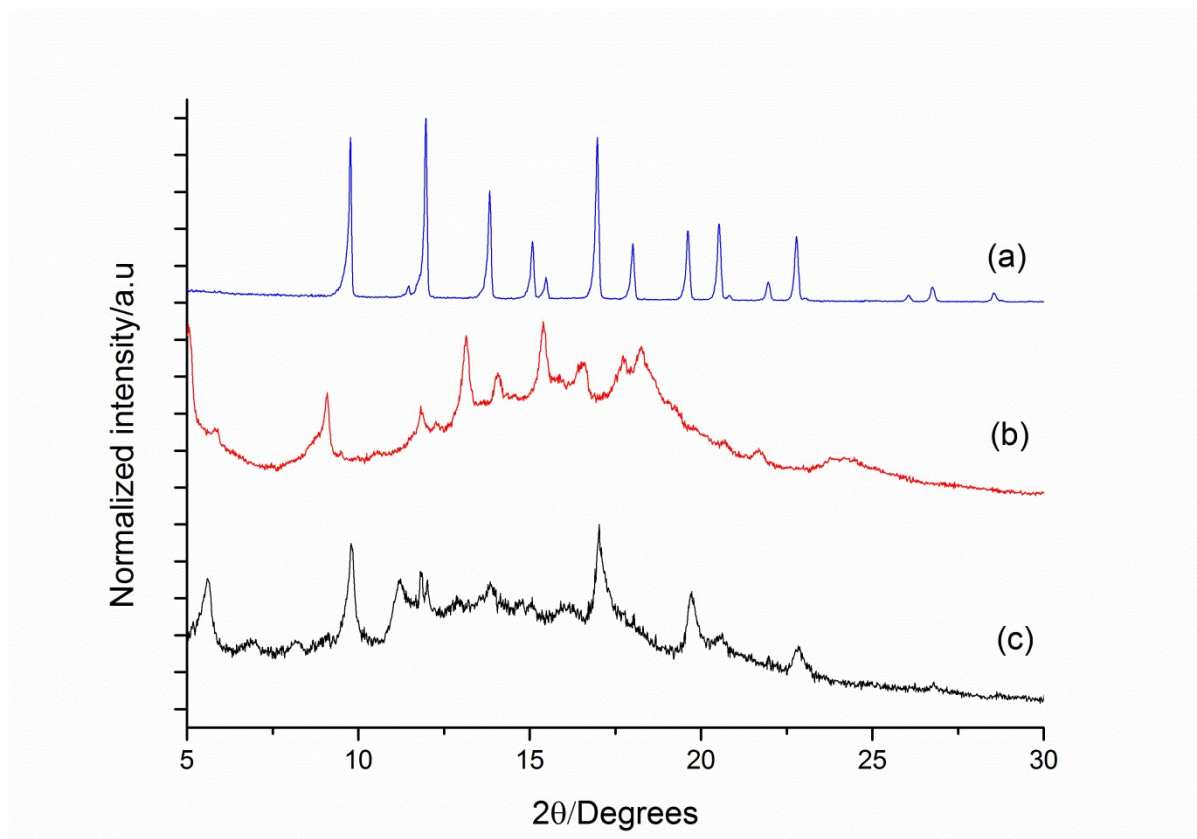


Figure S5. PXRD analysis of (a) **FT-RCC3-R**, (b) **CC13**, and (c) a phase mixture comprising **FT-RCC3-R** and **CC13**. All samples were crystallised from $\text{CH}_2\text{Cl}_2/\text{acetone}$.

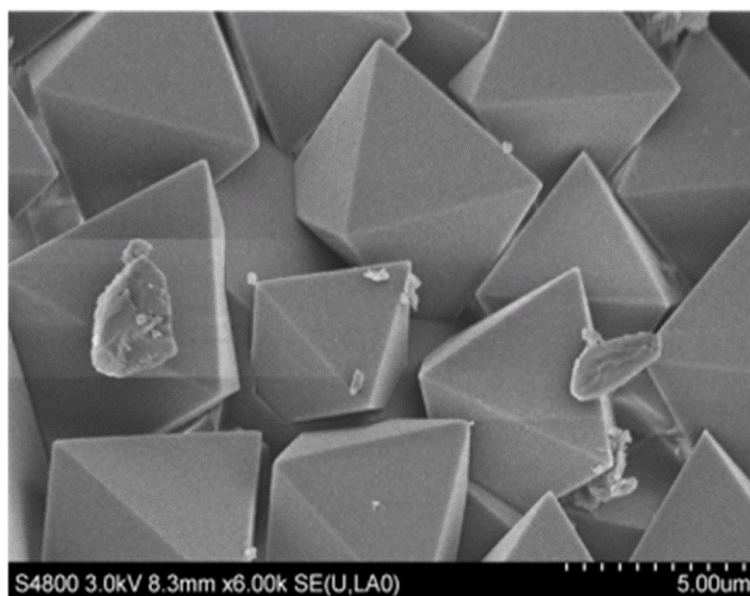


Figure S6. SEM image of ternary co-crystal, $(\text{CC3-}S_{0.5}\text{CC4-}S_{0.5}) \cdot (\text{CC13-}S_{0.5}\text{CC3-}S_{0.25}\text{CC4-}S_{0.25})$, displaying octahedral crystal habit.

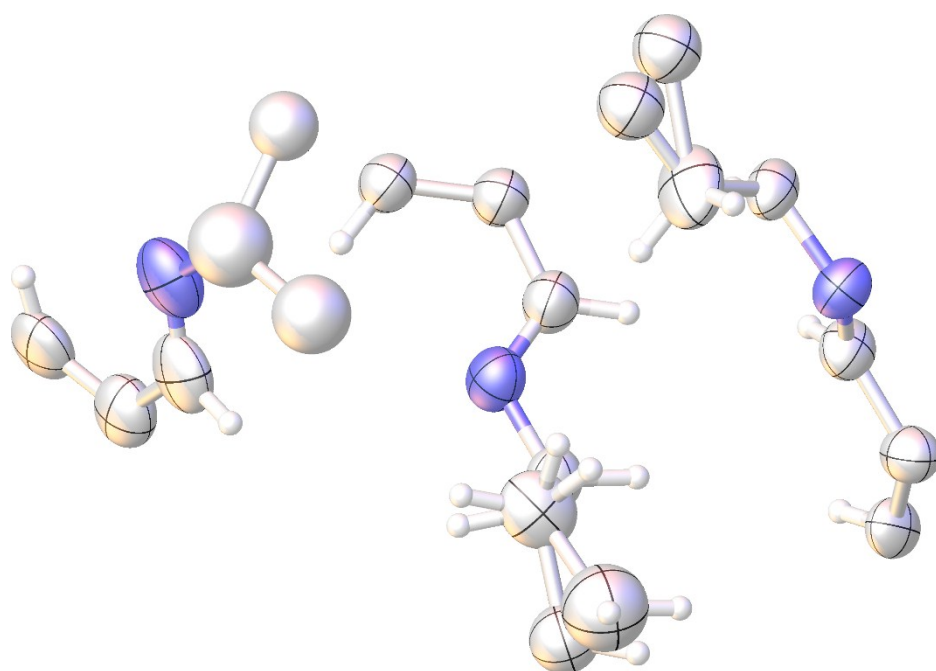


Figure S7. Displacement ellipsoid plot of the asymmetric unit from the single crystal structure, $(\text{CC3-}S_{0.5}\text{CC4-}S_{0.5})\cdot(\text{CC13-}S_{0.5}\text{CC3-}S_{0.25}\text{CC4-}S_{0.25})\cdot(\text{H}_2\text{O})_{11.92}$; residual H_2O omitted for clarity. Ellipsoid are displayed at 50% probability level. Isotropically refined C atoms shown as spheres. H-atoms for the severely disordered C-H groups were not all refined as part of the asymmetric unit but the appropriate number of H atoms were included in the refined formula unit.

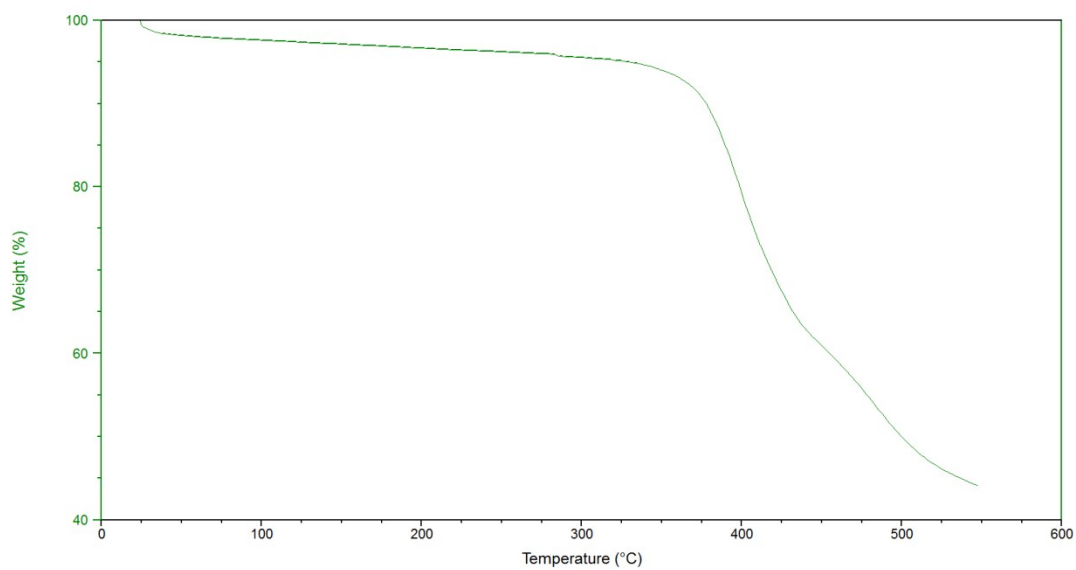


Figure S8. TGA for ternary co-crystal, $(\text{CC3-}S_{0.5}\text{CC4-}S_{0.5}) \cdot (\text{CC13-}S_{0.5}\text{CC3-}S_{0.25}\text{CC4-}S_{0.25})$, crystallised from $\text{CH}_2\text{Cl}_2/\text{acetone}$.

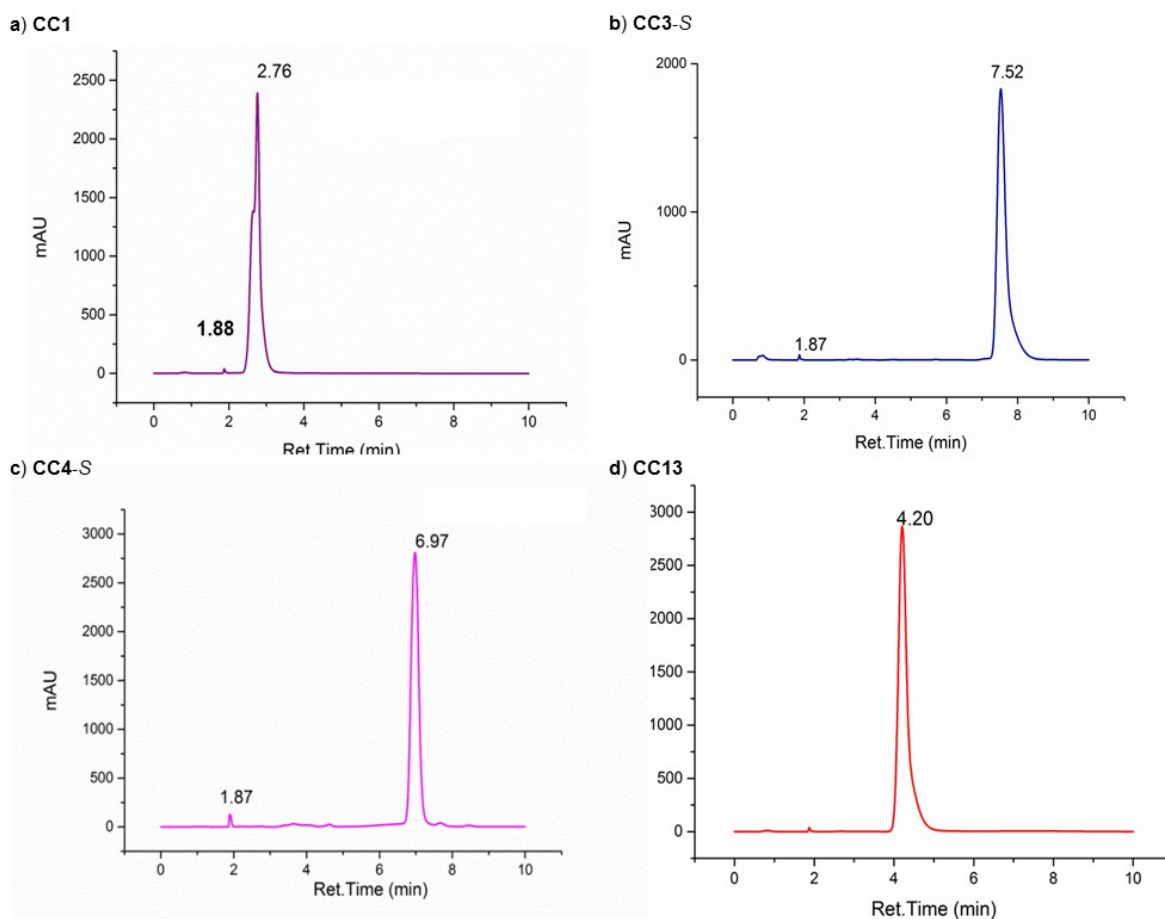


Figure S9. HPLC analysis for the single component cages **CC1** (retention time: 2.76 mins.), **CC3-S** (7.52 mins.), **CC4-S** (6.97 mins.), **CC13** (4.2 mins.) dissolved in CH_2Cl_2 (1.87 min). Column: Synchronis C8; 3 μm ; 4.6 \times 150 mm; mobile phase: isocratic MeOH; flow: 1.0 mL/min; oven temperature = 30 $^\circ\text{C}$; detection λ = 254 nm. (For all single component and co-crystals same conditions are used). For quantitative analysis, 0.047 M solutions of **CC1**, **CC13**, **CC4-S** and **CC3-S** were prepared. Each cage solution was diluted to X/2, X/3, X/4, X/5 and X/6 and HPLC analysis was collected. Peak areas were used to calculate calibration curves which were used to calculate the relative concentration of each cage in a crystalline solid.

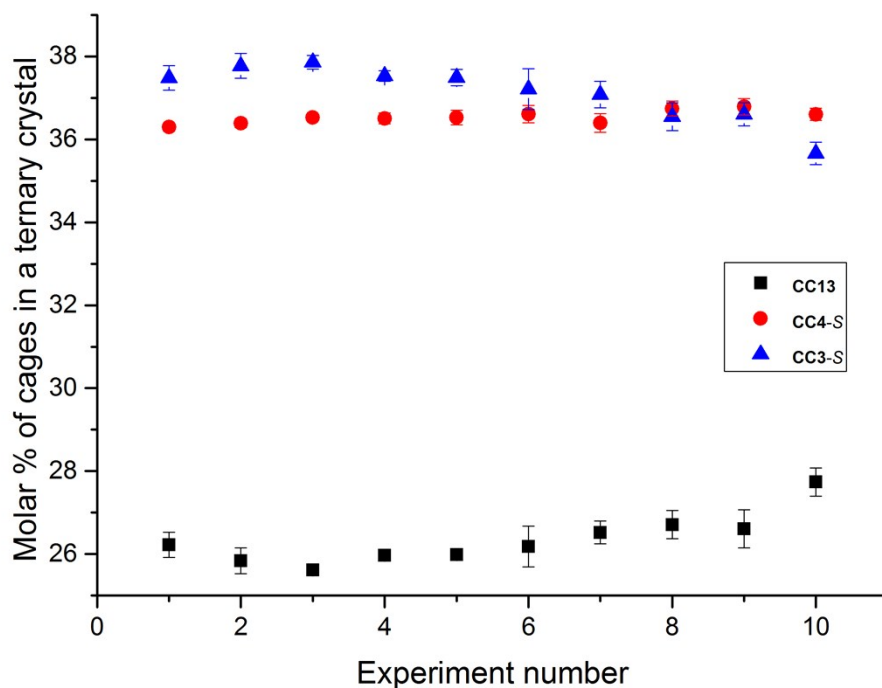


Figure S10. Quantitative HPLC analysis of ten single crystals of the ternary organic crystal, $(\text{CC3-}S_{0.5}\text{CC4-}S_{0.5}) \cdot (\text{CC13-}S_{0.5}\text{CC3-}S_{0.25}\text{CC4-}S_{0.25})$, crystallised from $\text{CH}_2\text{Cl}_2/\text{acetone}$. Triangles, circles, and squares represent percentage composition of **CC3-S**, **CC4-S**, and **CC13** respectively in the single crystals. The quantitative percentage composition of **CC3-S**, **CC4-S**, and **CC13** in the ternary crystals determined by HPLC analysis and is in good agreement with the refined single crystal structure.

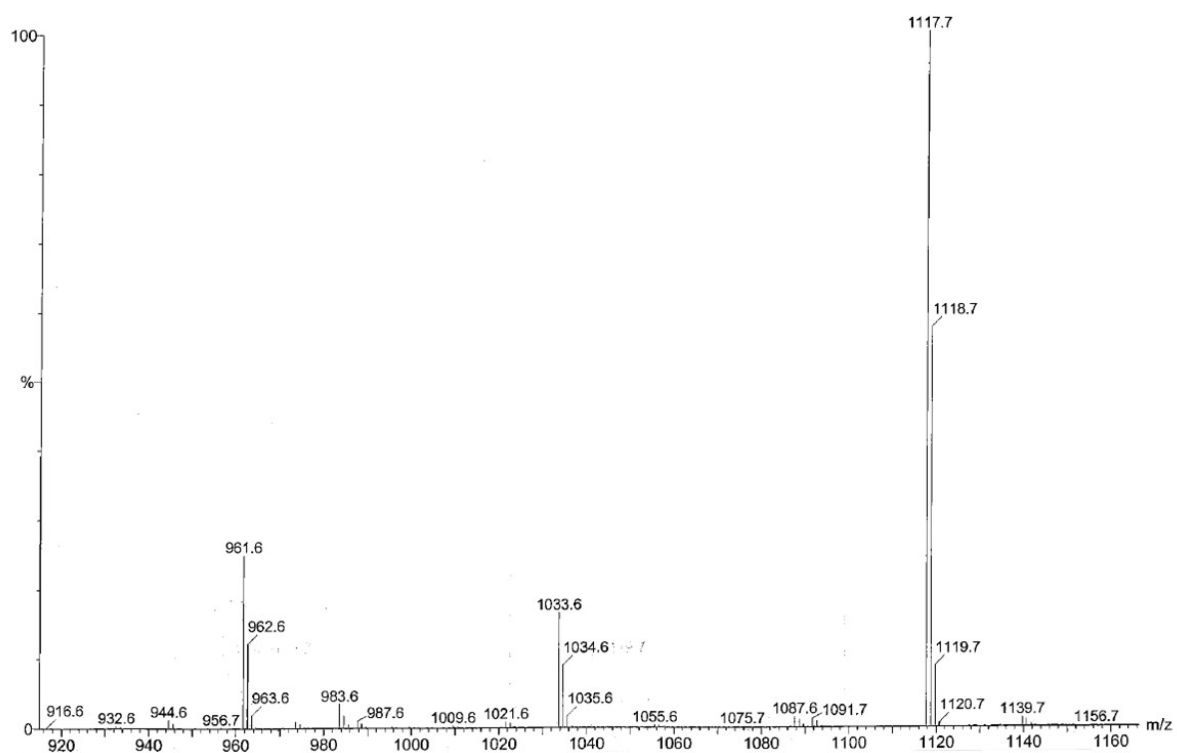


Figure S11. Mass spectrum for a single crystal of the ternary organic solid, $(\text{CC3-}S_{0.5}\text{CC4-}S_{0.5}) \cdot (\text{CC13-}S_{0.5}\text{CC3-}S_{0.25}\text{CC4-}S_{0.25})$ crystallised from $\text{CH}_2\text{Cl}_2/\text{acetone}$. m/z ratios correspond to: 961.6 $[\text{CC13}+\text{H}]^+$, 1033.6 $[\text{CC4-S}+\text{H}]^+$ and 1117.7 $[\text{CC3-S}+\text{H}]^+$.

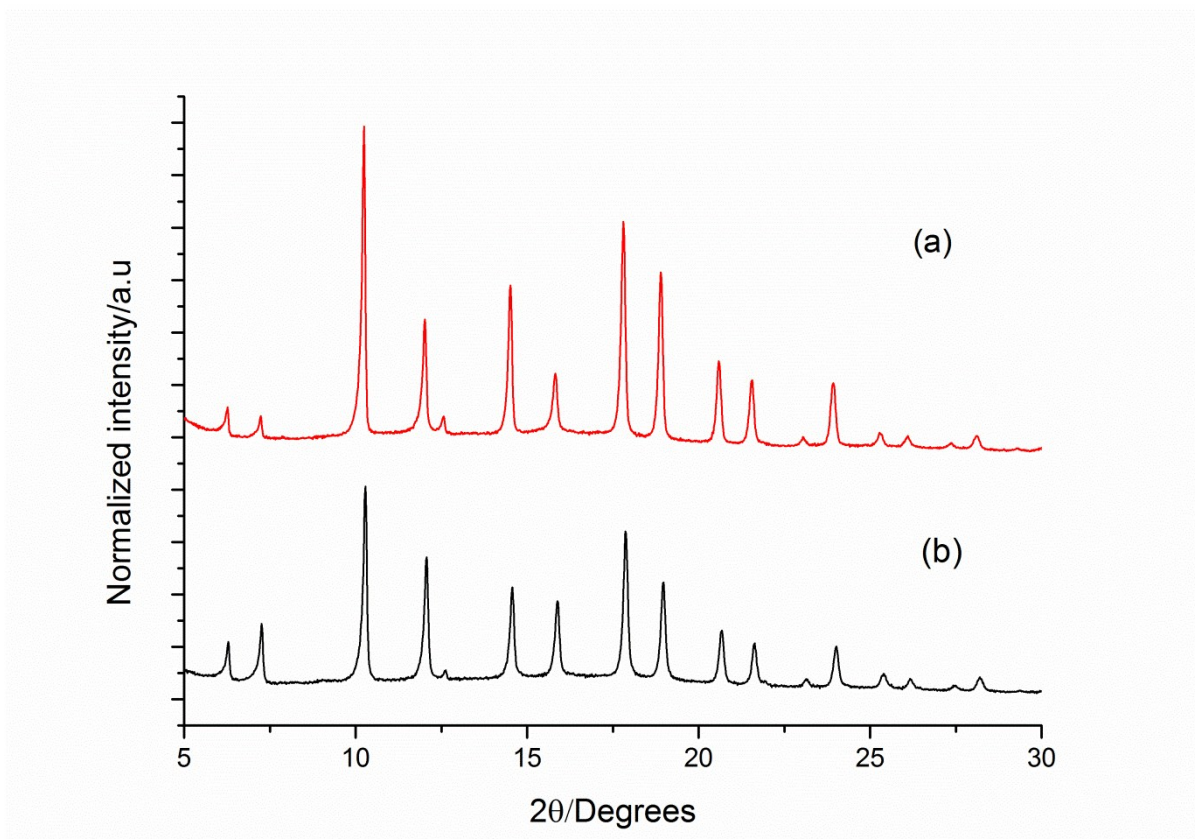


Figure S12. PXRD of ternary organic cocrystal, $(\text{CC3-}S_{0.5}\text{CC4-}S_{0.5})\cdot(\text{CC13-}S_{0.5}\text{CC3-}S_{0.25}\text{CC4-}S_{0.25})$, crystallised from $\text{CH}_2\text{Cl}_2/\text{acetone}$, recorded (a) before and (b) after gas sorption analysis.

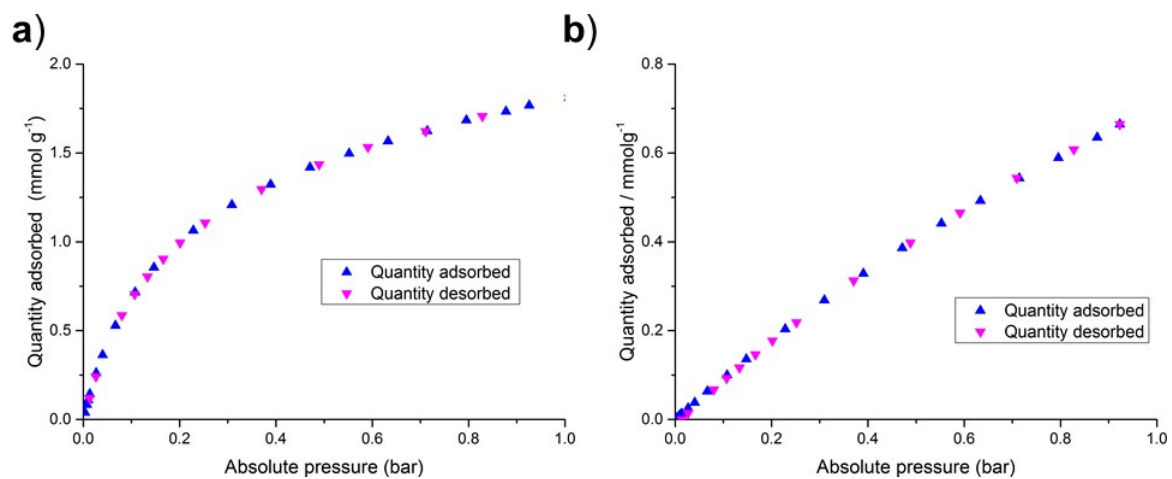


Figure 13. (a) Gas sorption analysis of ternary organic cocrystal, $(\text{CC3-}S_{0.5}\text{CC4-}S_{0.5})\cdot(\text{CC13-}S_{0.5}\text{CC3-}S_{0.25}\text{CC4-}S_{0.25})$, crystallised from $\text{CH}_2\text{Cl}_2/\text{acetone}$ for (a) Xe, and (b) Kr.